IJCRT.ORG ISSN : 2320-2882

INTERNATIONAL JOURNAL OF CREATIVE RESEARCH THOUGHTS (IJCRT)

An International Open Access, Peer-reviewed, Refereed Journal

An Efficient Electrocatalysts For Seawater Hydrogen Evolution Reaction

[1]Suraj Prajapati, [2]Dr. Dharmendra Singh,
[1]Master's Student, [2]Assistant Professor,
[1]Computational Science ,
[1]Central University of Punjab, Bathinda, India

Abstract: The severe operating conditions and requirement for highly potent and efficient electrocatalysts make the hydrogen evolution process (HER) in direct seawater electrolysis a major problem. In this work, (Mo) will be doped into a platinum-cobalt (PtCo) matrix to improve the catalytic activity of a new PtCoMo electrocatalyst for HER. The PtCoMo structure was optimized using the Atomic Simulation Environment (ASE) GUI, and its electronic characteristics were examined using Density of States (DOS) calculations with the Fermi level set to 0 ev. Minimal lattice deformation was seen in the optimized PtCoMo structure, suggesting that Mo was well incorporated into the PtCo matrix. The d-band center shifted closer to the Fermi level and the density of states near it increased, according to DOS analysis. The calculated binding energy of -2.8 eV indicates a strong interaction between Mo and the PtCo matrix, confirming the stability of the doped structure. Furthermore, the Gibbs free energy calculations demonstrated improved thermodynamic stability of PtCoMo at room temperature compared to doped PtCo. The self-supported Pt-Co-Mo electrode presents outstanding HER activity, which only requires extremely low overpotentials of 179.2 mV and 194.1 mV to reach a large current density of 2000 mA cm^{-2} in 1 M KOH and 1 M KOH seawater, respectively, for overall water splitting, cell voltages down to 1.50 V and 1.51 V are necessary to drive 10 mA cm^{-2} in 1 M KOH and alkaline seawater, respectively.

I. Introduction

Hydrogen is a clean energy that can address the energy crisis and environmental issues. One viable method for producing hydrogen is water splitting by electrolysis [1-3]. In recent decades, research has mostly concentrated on producing high-performance electrocatalysts for the hydrogen evolution reaction (HER) and oxygen evolution reaction (OER) in acidic or alkaline electrolytes with high-purity freshwater. Hydrogen is versatile and can enable renewables such as wind and solid photovoltaic (PV) to contribute more significantly. Hydrogen attempts have failed due to environmental factors caused by thermal processing. However, recent technological advancements include electric vehicles (EVs), wind, batteries, and solar PV. Policies have shown that they can create global clean energy industries. Clean hydrogen is gaining much attention and support, with increasing global projects and policies being developed. This is because hydrogen has the potential to address a range of energy challenges, such as reducing emissions, particularly in- industries like iron and steel, chemicals, and long-distance transportation, and it has a variety of uses and applications, for example, in the pro-duction of fertilizers and the oil refining sector [4]. Presently, great progress has been made for some electrocatalysts achieving performance even better than the commercial platinum (Pt) and iridium dioxide (IrO_2) [5]. In this context, the electrolysis of seawater, which is the most abundant water resource on earth (~97%), is highly intriguing for sustainable energy production [6]. Compared with the electrolysis of freshwater, the development of seawater electrolysis takes significant advantages in three aspects: (i) it makes full use of abundant seawater resources and avoids consuming precious freshwater resources, especially for those in arid regions; (ii) seawater is similar to a 0.5 M (KOH) aqueous solution with high ionic conductivity (33.9 mS cm^{-1} at 25 °C), avoiding the complex processes by adding alkaline or acidic species, thereby helps to reduce cost [7]. (iii) it is also a promising technology for seawater desalination when

it transforms the hydrogen back into electricity and water through combination of a direct seawater electrolyzer and a fuel cell [8].The first generation of hydrogen by electricity was per- formed as early as 1789 by van Troostwijk and Deiman using an electrostatic generator as the direct current source [9]. Various countries have formulated hydrogen energy development policies, which project that by 2030, global hydrogen demand will increase significantly and reach 115 million tons. (PEMWEs) are now the main commercial method of producing hydrogen and an (AWE). However, the development of "green hydrogen" technology is constrained because both approaches demand extremely pure water and use a significant amount of freshwater resources. The best resource for electrolysis is seawater, which makes up 96.5% of all the water on Earth. In particular, for some countries with coastlines and arid lands, such as Egypt and Iran, the utilization of seawater for hydrogen production is in line with national energy development strategies [10]. Seawater contains cationic heteroatoms like Mg^{2+} and Ca^{2+}, bacteria, and other microorganisms that reduce the long-term stability of membranes and catalysts This is especially true for the hydrogen evolution process (HER). Furthermore, the low levels of carbonate and borate ions in seawater result in poor conductivity, hindering the ability to maintain high current densities and slowing down HER kinetics. Recently, analytical research has shown that the combination of seawater reverse osmosis systems and conventional electrolyzers is a viable option for seawater electrolysis. However, they found that the cost of indirect seawater electrolysis was insignificant when compared to the cost of water electrolysis considering purification/desalination plants of seawater.This complicates the procedure overall in the interim, and technological issues still need to be resolved. Conversely, seawater's corrosive properties prevent direct electrolysis from producing hydrogen, despite its ability to do so in an effective and adaptable manner. This review presents the rationale and difficulties associated with direct seawater splitting and provides a detailed summary of the current strategies being used to address the issue. These strategies include the development of highly active, selective, and chemically stable catalysts; hybrid seawater electrolysis systems; corrosion-resistant seawater membranes; and self-powered seawater splitting systems [11]. Given the notable advancements seen in saltwater electrolysis in recent years, there is a demand to merge the latest advancements in the design approach for the fabrication of corrosion-resistant electrodes in the context of seawater electrolysis. AEMWE, a relatively recent electrolyzer technology, shows potential for significant advancements with ongoing investments and research. It offers environmental benefits by utilizing PGM-free electrocatalysts and fluorine-free polymeric membranes/ionomers for sustainable green hydrogen production. However, challenges in material stability, durability (especially at higher temperatures), and integration into MEAs need resolution. The durability issue involves mitigating degradation mechanisms and addressing complex interactions between materials, requiring strategic approaches. Ongoing research is crucial for understanding water transport, hydration effects, and catalyst-ionomer interactions, tailoring stability targets for different AEMWE configurations. A comprehensive method is essential to optimize the durability and performance of AEMWE systems [12]. The critical evaluation and comparison of the latest advancements in the areas of HER, OER, and bifunctional catalysts for direct seawater electrolysis in alkaline environments, have significant importance in addressing the challenges associated with seawater electrolysis. In recent years, a large number of HER and OER electrocatalysts with improved activity and durability performances, have been developed for application in direct seawater electrolyzers. The catalysts used in direct seawater electrolysis are thoroughly examined in this article, which also rates them according to overpotential and durability at current densities of 500 $mAcm^{-2}$ and 1000 $mAcm^{-2}$.The concluding section summarizes the findings presented in the preceding sections and presents the future outlook, explaining the potential implications of the discussed catalysts in advancing the field of direct seawater electrolysis for sustainable green hydrogen production. Furthermore, we offer a hypothesis aimed at reducing catalyst corrosion, which involves employing a molecular sieve approach to filter out chloride ions HER performance and durability in alkaline seawater [13].

Table: 1 list the HER, OER, and side reaction pathways associated with direct seawater electrolysis in an alkaline seawater environment [16]

Cathode	**HER in alkaline seawater media**		$2H_2O + 2e^- \rightarrow H_2 + 2OH^-$
	Volmer step–water dissociation (Catalyst Reduction)		$2H_2O + 2e^- \rightarrow 2H_{catalyst} + 2OH^-$
	Heyrovsky step (Catalyst Oxidation)		$H_2O + H_{catalyst} + e^- \rightarrow H_2 + OH^-$
	Tafel step (Catalyst Oxidation)		$2H_{catalyst} \rightarrow H_2$
	Ca^{+2} & Mg^{+2} precipitation		$M^{+2} + 2OH^- \rightarrow M(OH)_{2\ catalyst}$
Anode	**OER in alkaline seawater media**		$4OH^- \rightarrow O_2 + 2H_2O + 4e^-$
	Hydroxyl absorption		$OH^- \rightarrow OH_{catalyst} + e^-$
	Catalyst Oxidation		$OH_{catalyst} + OH^- \rightarrow O_{catalyst} + H_2O + e^-$
	Catalyst Hydroperoxidation		$O_{catalyst} + OH^- \rightarrow OOH_{catalyst} + e^-$
	Catalyst Reduction		$OOH_{catalyst} + OH^- \rightarrow O_2 + e^- + H_2O$
	Side reactions in alkaline seawater media at overpotential>490 mV		$Cl^- + 2OH^- \rightarrow 2ClO^- + H2O + 2e^-$
	Volmer step- Chloride adsorption		$Cl^- \rightarrow Cl_{catalyst} + e^-$
	Volmer step- Chloride adsorption		$O_{catalyst} + Cl^- \rightarrow OCl_{\ catalyst} + e^-$
	Tafel step (Chlorine formation)		$2Cl_{catalyst} + 2Cl^- \rightarrow Cl_2 + 2e^-$
	Hypochlorite formation (In the Anolyte)		$Cl_2 + 2OH^- \rightarrow 2OCl^- + H_2O$
	Catalyst Corrosion		$Cl_{catalyst} + x\ Cl^- \rightarrow M(Cl)_x^-$

The impact of OH and Cl concentrations on the activity and stability of the OER and HER catalysts is of particular interest for direct seawater electrolysis. As shown in Table 1, hydroxyl ions are formed during the HER, which increases the pH and negatively impacts the activity of the cathode. Conversely, the OER activity of the anode catalyst is enhanced by increasing the OH concentration (see Table 1). At high pHs, the mechanism for HER follows two well-known steps, Volmer-Tafel and Volmer-Heyrovsky [14]. At the anode side, unwanted side reactions leading to CER can occur at overpotentials above 490 mV. The chlorine species generated during CER can oxidize and poison metal species present in both catalysts and cell hardware, resulting in reduced efficiency and stability of cells. Hence, choosing the right catalyst that can maintain the overpotential below 490 mV is essential to maintain OER selectivity over CER (Chlorine Evolution Reaction) (see Table 1) [15]. It has been claimed that some electrocatalysts, specifically transition metals doped with nitrogen, are appealing choices for direct seawater splitting. The advancement of highly efficient catalysts for the HER is of importance in achieving optimal energy efficiency across diverse applications. For advanced HER catalysts, it is traditionally observed that the primary choice among the electrochemical community revolves around utilizing Pt. However, there has been a joint effort to delve into cost-effective alternative sources that are abundantly available [17].

2. Fundamentals and challenges of seawater splitting

2.1. Electrode reactions and challenges for water splitting

The OER at the anode and the HER at the cathode are the two half-reactions that make up water splitting. The HER is a two-electron-proton transferring process, while the OER is a multi-electron transferring process, combining several intermediates and the removal of four protons per oxygen molecule. According to the electrolytes, water splitting follows different redox reactions. In acidic electrolytes, the overall redox reactions can be expressed by equation [18,19].

$$\text{Cathode: } 2H^+ (aq) + 2e^- \rightarrow H_2 (g) \quad (2.1)$$

$$\text{Anode: } H_2O (l) \rightarrow 2H^+ (aq) + O2 (g) \frac{1}{2} O_2 (g) \quad (2.2)$$

In alkaline electrolytes, the redox reactions can be expressed by Equation

$$\text{Cathode: } 2H_2O (l) + 2e^- \rightarrow 2OH^- (aq) + H_2 (g) \quad (2.3)$$

$$\text{Anode : } 2OH^- (aq) \rightarrow H_2O (l) + 2e^- + \frac{1}{2} O_2 (g) \quad (2.4)$$

For the neutral seawater electrolysis, the redox reactions are believed similarity to those in alkaline electrolytes, that is, it involves water decomposition to OH^- and hydrogen at the cathode. However, the anodic reaction is complex due to the competition reaction of Cl^- oxidation with the OH^- oxidation, which will be discussed in detail later. At the standard condition, the change in Gibbs free energy (ΔG) for water electrolysis is 237.2 kJ mol^{-1}, corresponding to an equilibrium potential of 1.23 V. However, in practice, the water electrolysis requires a voltage larger than 1.23 V due to the existing kinetic barriers and poor energy efficiency in both the cathodic and anode sides. Though water electrolysis can be easily achieved on catalytic electrode materials, some disadvantageous factors like high activation energy, low ion, and gas diffusion rates, and some factors related to the electrolysis system such as solution concentration, wire and electrode resistances, electrolyte diffusion blockage, etc. leading to either large overpotentials or poor durability for water splitting. Therefore, the main challenge in water electrolysis is to design scalable electrocatalysts with excellent efficiency and durability [20]. To be specific, with the electrolysis current increasing, the local pH value near the electrode surface would dramatically increase so may result in the formation of $Ca(OH)_2$ and $(Mg(OH)_2$ precipitation[21] and block the cathode active sites Mayrhofer et al. pointed that even at moderate current densities, the pH values near the electrode surface could increase 5–9 pH units from that of a slightly buffered medium with near-neutral bulk pH of 4–10 [fig.1] [22]

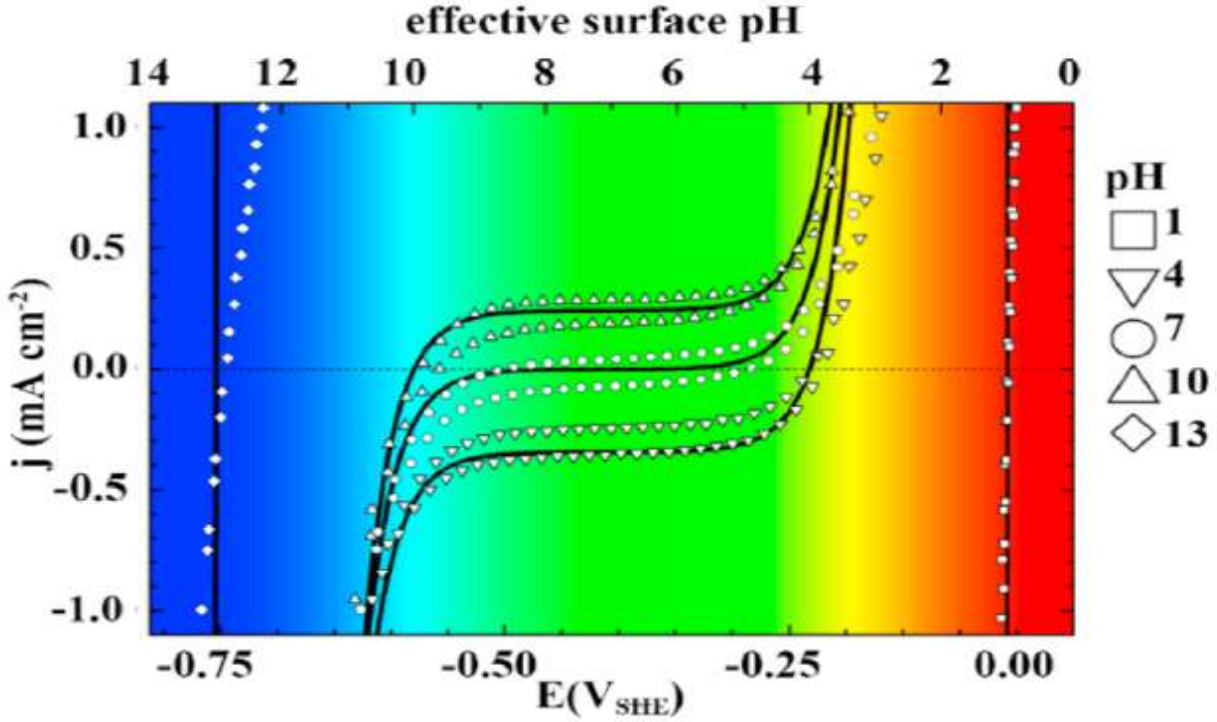

Fig.1: The current density-surface pH relation established from cyclic voltammetry in H_2-saturated, unbuffered solutions of bulk pH 1–13 [22].

To address such dramatic pH fluctuations, a buffer solution or additives to stabilize the pH fluctuations is required for current seawater electrolysis systems. Besides, other strategies like designing appropriate electrolysis cells and membranes to separate the $Ca(OH)_2$ and $(Mg(OH)_2$ precipitation from the cathodes might be also possible to overcome this challenge. In addition, the cathodic competing reactions involving the dissolved metal ions (such as Na^+, Cu^{2+}, and Pb^{2+}) may also occur depending on the applied electrolysis potentials(see Fig.2a)[26]. Therefore, it is essential to limit these undesirable electrochemical processes to build powerful electrocatalysts for HER in seawater. In this regard, adopting a suitable membrane to separate the catalyst from the seawater source (Fig. 2b), developing catalysts with inherent corrosion resistance or selective surface chemistry (Fig. 2c), or using blocking layers like perm-selective barrier layers attached to the catalysts (Fig. 2d) are considered as potential solutions to improve the long-term stability of HER electro-catalysts in seawater [26]. For the anode electrode, seawater contains large quantities of electrochemically active anions (such as Cl^-) that would interfere and compete with the anodic OER. Taking into account all anions with their corresponding standard redox potentials, the chloride chemistry would compete with the OER at the anode during seawater electrolysis. This key challenge has long been identified and discussed by Bennett in 1980 [27,28] He found that though the direct electrolysis of seawater could result in the cathodic evolution of hydrogen at high current efficiency, large amounts of chlorine in the form of hypochlorite solution normally evolved at the anode. The chloride chemistry in aqueous is complicated and several possible reactions could occur depending on the pH, applied potentials, and the concentration of chloride ions. After a thorough examination of anodic seawater electrolysis and its drawbacks, Strasser et al. provided a computed Pourbaix diagram that included the OER and the chloride chemistry. both the ClER and the hypochlorite formation are two-electron reactions, which are kinetically favorable compared with the four-electron response from OER. Even though the thermodynamics favors the OER, the kinetics is much faster for the ClER, which leads to the commonly observed higher overpotential for OER than ClER. Therefore, developing electrocatalysts of high selectivity for OER is essential to avoid ClER and hypochlorite formation during the direct electrolysis of seawater.

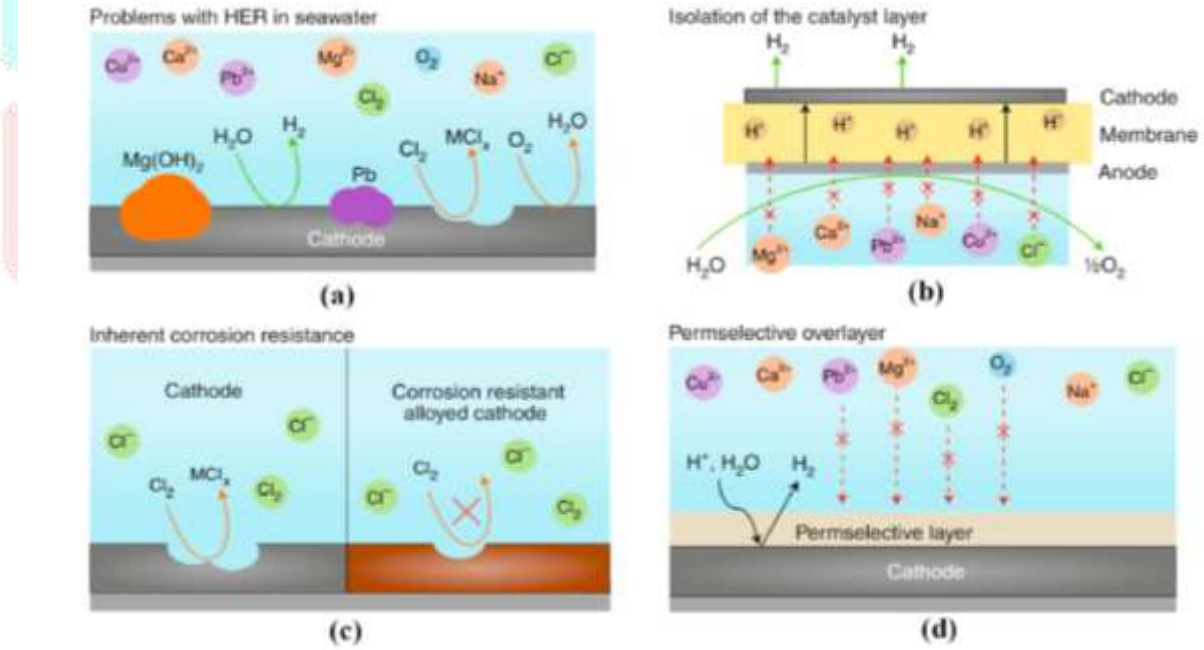

Fig. 2. Challenges and potential solutions to improve the long-term stability of HER in seawater [26].

2.2. Electrolyzer design for water splitting

For the application of water electrolysis, apart from developing highly efficient catalysts with long durability, it is essential to design an appropriate electrolyzer with high performance and low cost. The four most common configurations for water electrolysis at the moment are (PEMWE), (AEMWE), (AWE), and (HTWE), which can perform solid oxide electrolysis (~800–1000°C) and proton-conducting ceramic membrane electrolysis (~150–400°C) [23-25], as shown in (Fig. 3).

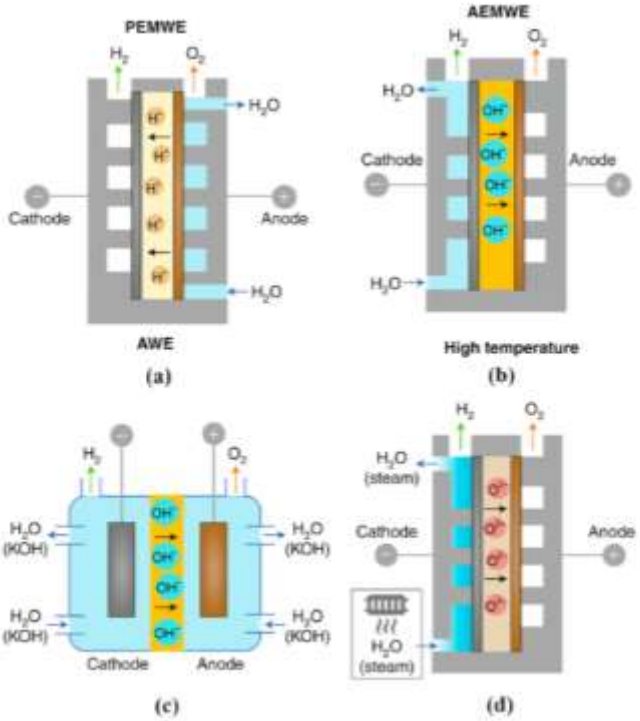

Fig. 3. Configurations for water electrolysis: (a) (PEMWE), (b) (AEMWE), (c) (AWE), (d) (HTWE) [26].

Generally, the four leading configurations are designed for freshwater-based electrolysis, which can be directly used as seawater electrolyzers. However, the above four configurations share common problems, which mainly result from the complicated compositions of natural seawater. Therein, the physical/chemical interferences of the ion exchange membranes and the corrosion of metal components are the main concerns for seawater electrolysis. For example, contaminating cations, such as Na+, $Mg^{2+,}$ and Ca^{2+} in seawater, could degrade the performance of proton exchange membranes (PEMs) in PEMWE and HTWE [29]. The additional anions in seawater, such as Cl^-, Br-, and $SO_4^{2-,}$ could negatively influence the membrane performance in AEMWE, AWE, and HTWE [30,31]. In addition to the existing ions, bacteria/microbes and solid impurities/precipitates in seawater could also lead to either low efficiency or physical/chemical interferences to the electrolysis components due to physical blockages. It is worth mentioning that the stability of the ion exchange membranes also influences the lifetime of seawater electrolyzers. As mentioned above, the contaminating cations in seawater could degrade the membrane's performance; therefore, developing stabilized membranes in seawater is also a challenging yet important task for direct seawater electrolysis. In this respect, the pre-filtration of the seawater is necessary for direct seawater electrolyzers. To this end, a simple filtration of natural seawater using membrane filtration techniques such as microfiltration or ultrafiltration is capable of largely solving the problem related to the physical blockages from solid impurities, precipitates, and microbial contaminations affecting either the catalysts or membranes in the electrolyzers. By performing a simple filtration of the natural seawater, an improved long-term durability of the electrolyzer could be achieved. Also, to reduce the risk of metal component corrosion in electrolyzers, the current collectors and separator plates that are made of titanium, graphite, or stainless steel are preferred [32], while the lifetime of these materials under seawater situations should be carefully considered.

2.3 Electrolyser efficiency for water splitting

To understand the electrolyzer efficiency (there is also electrolyzer system efficiency which is lower by around 10%, mostly from power conversion) and power consumption of the water electrolysis process, the thermodynamics of the water splitting process must be explained. At standard conditions, the reaction is nonspontaneous (□□ = 237 kJ mol^{-1}) and the useful work is equal to the change in Gibbs energy [33, 34]. Faraday's law is used to relate the electrical energy required for the electrochemical conversion where the reversible voltage (□rev) is:

$$E_{rev} = \frac{\square\square}{\square\square} \quad (2.3.1)$$

Where □ is the number of electrons transferred and □ is the charge transferred per mole of electrons (□ = 96,485 C mol^{-1}). The Gibbs free energy change is defined by the enthalpy change minus the irreversibility (□ Δ□) [33], and so the thermoneutral cell voltage is:

$$E_{tn} = \frac{\square\square}{\square\square} \quad (2.3.2)$$

At standard conditions, the reversible and thermoneutral voltages are
1.229 V and 1.482 V, respectively.

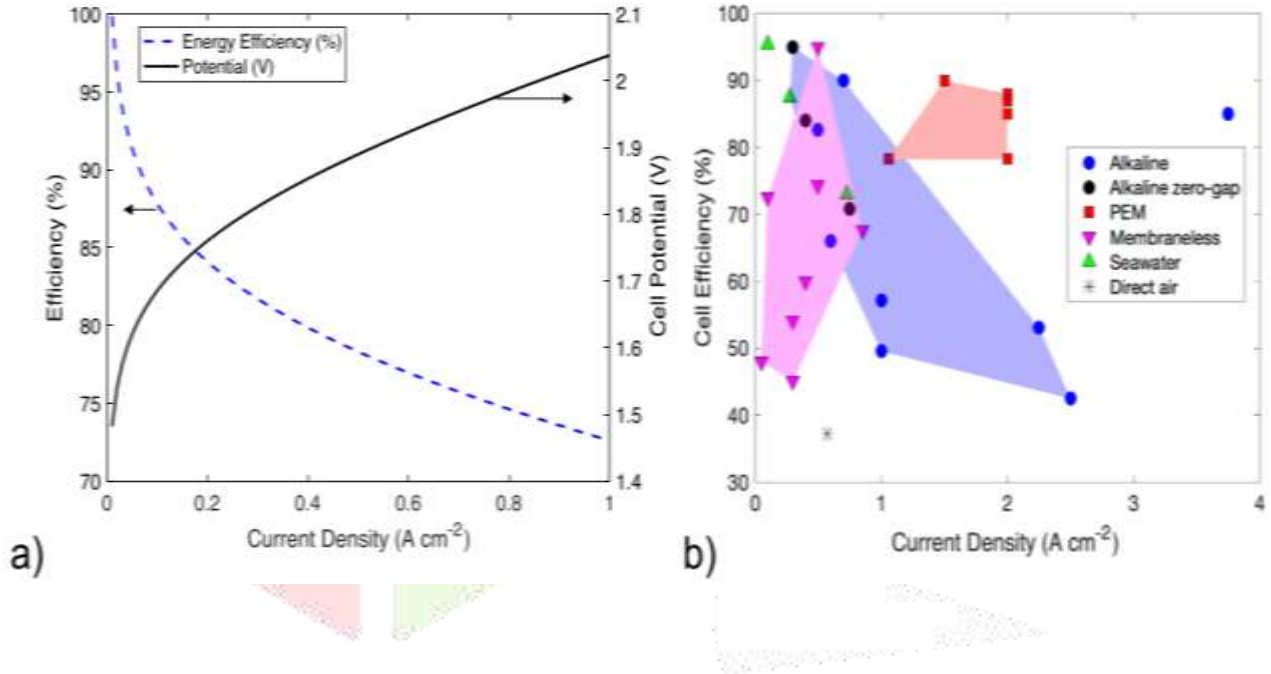

Fig.: 4 (a) Example characteristic curve of the effect of increasing the current density on the cell potential and corresponding efficiency at standard conditions (room temperature). (b) extracted cell efficiency for electrolyzer literature evaluated in this study that reported potential or efficiency with regions for alkaline, PEM, and membrane-less highlighted in blue, red, and magenta respectively [35].

At higher temperatures, the reversible voltage can decrease and at higher pressures, it can increase. The energy efficiency of electrolysis (also shown in Fig. 4) is defined by the ratio between the operating voltage and the thermoneutral voltage,

$$\square = \frac{\square\square\square}{\square\square\square\square\square} \quad (2.3.3)$$

or in other words the chemical energy of hydrogen produced (39.4 kWh kg^{-1}) over the electrical energy used to generate hydrogen in the electrolyzer (43–58 kWh kg^{-1}). It should be noted that electrolyzer system efficiency is lower due to additional losses of 5–8 kWh kg^{-1} from power conversion/rectifier and balance of plant e.g. cooling fan and hydrogen loss such as through purification steps [35].
There are some formulas that are used to calculate the efficiency of an electrolyzer. The energy efficiency of the electrolyzer can be determined using the formula:

Energy Efficiency (%) = (□□ / □□□□□ □△□) □ 100 (2.3.4)

The measured current and Faradaic efficiency [35] to calculate the hydrogen production rate

$$HPR = \left(\frac{I \times Faradaic\ Efficiency}{2 \times F}\right) \quad (2.3.5)$$

Where I is the current, F is the Faraday constant, and $Faradaic\ Efficiency$ is the formula :

$$FE(\%) = \left(\frac{Actual\ amount\ of\ gas\ collected}{Theoretical\ amount\ of\ gas\ produced\ based\ on\ charge\ passed}\right) \times 100 \quad (2.3.6)$$

3.METHODOLOGY

3.1 System Preparation for Mo-Doped PtCo (PtCoMo) Electrocatalyst

3.1.1 Model Construction Using ASE GUI

This section details the methodology used to identify and study a suitable electrocatalyst for Hydrogen Evolution Reaction (HER) in direct seawater electrolysis, focusing on Mo-doped PtCo The methodology combines computational and experimental methods to guarantee a thorough comprehension of the catalyst's characteristics and performance. Begin with the creation of the base PtCo alloy structure using the Atomic Simulation Environment (ASE) GUI. Ensure that the initial atomic positions and lattice parameters correspond to a well-defined PtCo crystal structure. Procedure: Open ASE GUI and construct the PtCo crystal structure. Set the lattice parameter (angstrom)
Crystallographic data for PtCo. Populate the lattice with Pt and Co atoms in the correct stoichiometric ratio (18 Pt: 9 Co). Doping Process: Introduce Mo doping by substituting one Pt atom with a Mo atom within the PtCo lattice.
Procedure: Select a Pt atom within the constructed PtCo structure. Replace the selected Pt atom with a Mo atom to create the Mo-doped PtCo structure (see Fig. 5a). Ensure the dopant position is chosen to maintain structural integrity and is representative of the desired doping level. The atomic position (angstrom) [Mo 1.5707220644(a) 2.7205704201(b) 0.0000000000(c)].
Visualization and Editing: Use the ASE GUI to visually inspect the atomic arrangement and verify the correct placement of the Mo dopant [see Fig. 5b]

Procedure: Rotate and zoom into the structure to check for any irregularities or clashes caused by the substitution. Adjust the atomic positions if necessary to relax the initial strains introduced by the doping. Populate the lattice with Pt, Co, and Mo atoms in the correct stoichiometric ratio (17Pt: 9Co: 1Mo).

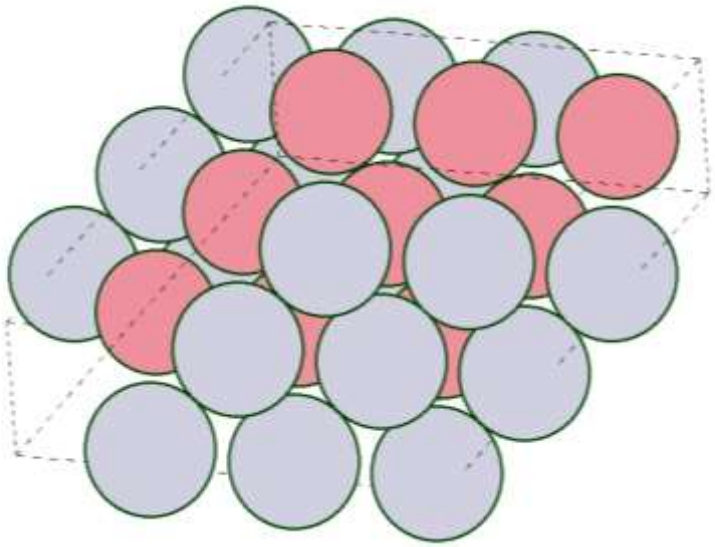

Fig: 5a The lattice with Pt and Co atoms in the correct stoichiometric ratio (18Pt: 9Co) using ASE GUI. Grey color (Pt) and Orange color (Co). Hexagonal lattice structure.

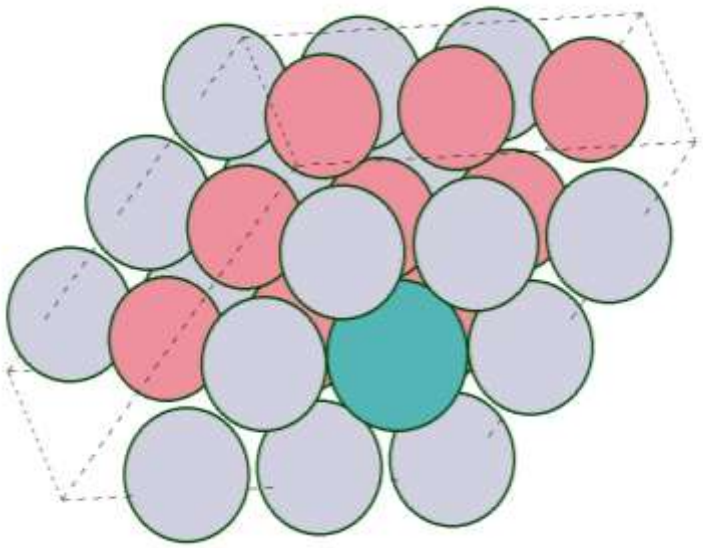

Fig: 5b The lattice with Pt, Co, and Mo atoms in the correct stoichiometric ratio (17Pt: 1Mo: 9Co) using ASE GUI. Grey color (Pt), Orange color (Co), and Green color (Mo) Hexagonal lattice structure(After Editing and visualization)

3.1.2 Atomic Coordinates and Cell Parameters Atomic Coordinates:

Export the atomic coordinates of the Mo-doped PtCo structure for use in subsequent computational simulations. Procedure: Use the ASE GUI to generate a file containing the atomic coordinates in a format suitable for the DFT software package (e.g., input files for Quantum ESPRESSO or GPAW, see in the appendix). Ensure all atoms' coordinates are correctly listed and formatted. With k-points (3 3 3 0 0 0) and lattice plane (1 1 1). Cell Parameters: Define the unit cell parameters that accommodate the Mo-doped structure, ensuring periodic boundary conditions if necessary.

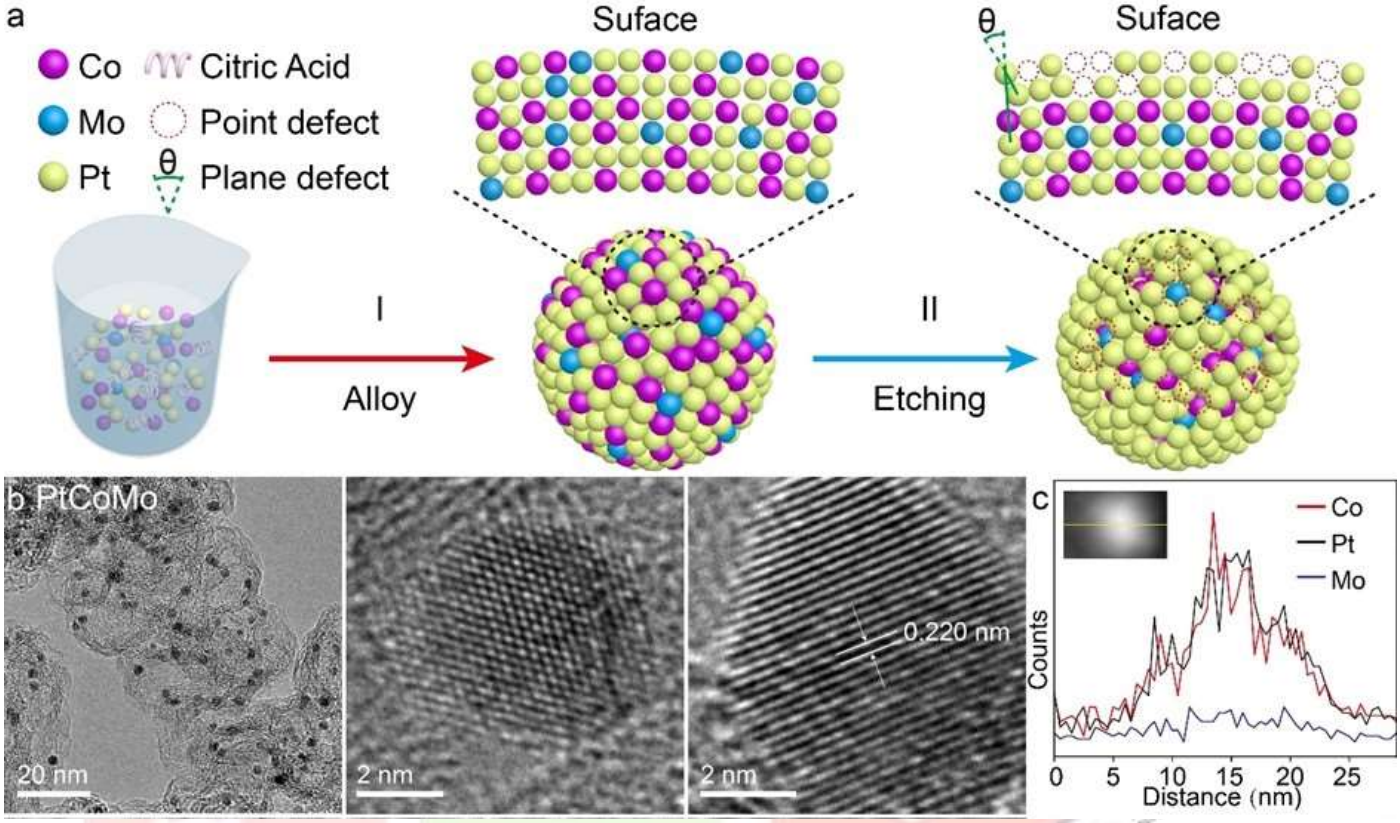

Fig: 8 The strategy for synthesizing V_{Co-Mo}-PtCoMo nanocatalysts. (a) The schematic diagram for the synthesis of V_{Co-Mo}PtCoMo nanocatalysts. (b) TEM and HR-TEM images of PtCoMo nanocatalysts without defects supported on carbon black. [52]

Procedure: Confirm the lattice vectors and cell dimensions are correctly set in the ASE GUI.

Table: 2 CELL_PARAMETERS (angstrom) of the PtCoMo (HER Catalyst)

a	b	c
8.0779992 *Å*	0.0000000 *Å*	0.0000000 *Å*
-4.0389996 *Å*	6.99575251895037 *Å*	0.0000000 *Å*
0.0000000 *Å*	-0.0000000 *Å*	4.27570618057627 *Å*

Check that the unit cell is large enough to prevent interactions between periodic images of the Mo dopant if using periodic boundary conditions. Adjust the cell parameters if required to balance computational efficiency and accuracy. using space group ($R\bar{3}m$).

3.2 HER Electrocatalysts for Seawater Electrolysis

Developing highly active and durable catalysts for the HER is essential to optimize the energy efficiency of the direct seawater electrolyzers. HER catalysts with reliable performance and durability are traditionally developed by using platinum. However, there is a rising need to investigate more affordable and widely accessible alternatives because of the restricted supply and high cost of Pt [36]. The utilization of composite electrocatalysts, comprised of both noble and non-noble metals, presents a promising avenue for achieving enhanced HER performance, thereby reducing the consumption of precious metals. Catalysts composed exclusively of non-noble metals have gained significant attention in the field of both conventional water electrolyzers and alkaline seawater electrolyzers. This increased interest indicates their potential suitability for application in large-scale H_2 production systems. However, there is a rising need to investigate more affordable and widely accessible alternatives because of the restricted supply and high cost of Pt. HER performance and durability in alkaline seawater. Certain electrocatalysts, namely nitrogen-doped transition metals, are reported to be attractive options as catalysts for direct seawater splitting (see Table 3). This attractiveness has been attributed to their good electrical conductivity and [37-39] corrosion resistance. The improved performance of the doped transition metals is explained by the structural and electronic changes that are induced by the non-metal component. The incorporation of Nitrogen or phosphorus within metal structures results in a reduction of the metal content, thereby altering the behavior of phosphides to resemble that of hydrogenase rather than a pristine metal surface. Moreover, the rational kinetics of hydrogen activation can be attributed to the capability of the negatively charged nitrogen atoms to effectively draw electrons from metal atoms, thus functioning as Lewis bases that effectively capture protons. The presence of a substantial energy barrier for water dissociation coupled with insufficient hydrogen desorption poses significant challenges in the pursuit of nitrogen-doped metals as catalysts for the HER in alkaline media. Consequently, enhancing the inherent characteristics of electrocatalysts utilized in alkaline HER necessitates the adjustment of water adsorption and dissociation binding energies in a mutually beneficial manner. The advancement of highly efficient catalysts for the HER is of importance in achieving optimal energy efficiency across diverse applications. For advanced HER catalysts, it is traditionally observed that the primary choice among the electro-chemical community revolves around utilizing Pt. However, there has been a joint [40-42] effort to delve into cost-effective alternative sources that are abundantly available. Table 2 shows a comparison of the performance of the-state-of-art HER cathode catalysts, evaluated in direct seawater electrolysis.

Table : 3 A comparative analysis of the overpotential and endurance of the most advanced saltwater electrolysis (SOA) HER cathode catalysts at varying current densities.

HER Catalyst	Electrolyte	Overpotential	Max Current Density	Durability	Ref.
NiMoN	1 M KOH and alkaline seawater	82 mV at (100 cm^{-2}) 160 mV at (500 cm^{-2}) 218 mV (1000 cm^{-2})	(1000 cm^{-2})	100 hrs At 25 ° C 600 hrs At (100 mA cm^{-2})	[43]

Cu_2S_2Ni	Alkaline seawater	200 mV at (500 mA cm^{-2})	500 mA cm^{-2}	150 h at (400 cm^{-2})	[44]
Ni-W_2 N	1 M KOH and alkaline seawater	265 mV at 500 mA cm^{-2} 310 mV at 1000 mA cm^{-2} 345 mV at 1500 mA cm^{-2}	1500 mA cm^{-2}	80 hrs 500 (mAcm^{-2})	[45]
Ni-MoN	1 M KOH and alkaline seawater	29 mV at 10 mA cm^{-2} 66 mV at 100 mA cm^{-2} 128 mV at 500 mA cm^{-2}	500 mA cm^{-2}	Stability: after 48000 cycles of CV no signifi-cant increase in the potential was observed	[46]
P-Ni_4-Mo	1 M KOH and alkaline seawater	260 mV at 100 mA cm^{-2} 551 mV at 1000 mA cm^{-2}	1000 mA cm^{-2}	more than 200 hrs	[47
B-Ni_2P-MoO_2	1 M KOH + seawater	29 mV at 10 mA cm^{-2} 50 mV at 50 mA cm^{-2} 64 mV at 100 mA cm^{-2} 91 mV at 200 mA cm^{-2} 496 mV at	500 mA cm^{-2}	more than 140 hrs	[48]

		500 mA cm^{-2}			
HW-$NiMoN_2$ h	1 M KOH + seawater	26 mV at 10 mA cm^{-2} 32 mV at 50 mA cm^{-2} 43 mV at 100 mA cm^{-2} 57 mV at 200 mA cm^{-2} 87 mV at 500 mA cm^{-2} 132 mV at 1000 mA cm^{-2}	1000 mA cm^{-2}	Over 70 hrs at 1000 mA cm^{-2}	[49]
NiRh Cu NA/CF	1 M KOH + seawater	155 mV at 300 mA cm^{-2}	300 mA cm^{-2}	over 30 hrs at 300 mA cm^{-2}	[50]
Pt-Co-Mo	1 M KOH and Alkaline seawater	25 mV at 100 mA cm^{-2} 74 mV at 500 mA cm^{-2} 117 mV at 1000 mA cm^{-2} 194.1 mV at 2000 mA cm^{-2}	2000 mA cm^{-2}	100 hrs stability test	[51]

3.3 Computational Study

3.3.1 Structural Optimization

Structural optimization (see Table 5) of a doped material like PtCo with Mo doping involves calculating the optimal atomic positions that minimize the system's total energy. DFT and QE are two computational chemistry programs that are commonly used in this process.

Here's a detailed description of the results you might obtain from such an optimization, Lattice parameters: Initial Structure: The PtCo initial crystal structure specifies the lattice parameters (a, b, c) (see in table 2) and angles (α, β, γ). For instance, PtCo might have a face-centered cubic (fcc) structure with lattice constant a. Here we use the Pt-Co-Mo to have a hexagonal structure with a lattice parameter (alat) = 15.2652 Bohrs The Atomic position of the PtCoMo are got by using the Ase Gui (software)(see table 6)

Table: 5 Optimization of Pt-Co-Mo catalyst

Atomic species	valence	mass	pseudopotential
Co	17.00	58.93319	Co(1.00)
Pt	16.00	195.08400	Pt(1.00)
Mo	14.00	95.95000	Mo(1.00)

\

Table: 6 Atomic position of Pt-Co-Mo catalyst

Wyckoff	Element	x	y	z
4 f	Pt	3/2	5/2	7/2
2p	Co	0	1/2	3/2
3d	Mo	1/2	3/2	5/2

After optimization, these parameters might slightly change to accommodate the Mo doping. For example, lattice constants might increase or decrease depending on the atomic radii and bonding nature of Mo relative to Pt and Co. Atomic positions are set according to the crystallographic positions of Pt and Co atoms(see Fig. 6). Doping Mo involves substituting some of these positions with Mo atoms (see in fig. 5b).

The positions of all atoms, including Mo, Pt, and Co, adjust slightly to achieve a kinetic-energy cutoff = 30.0000 Ry configuration. This might lead to a slight distortion of the initial lattice.

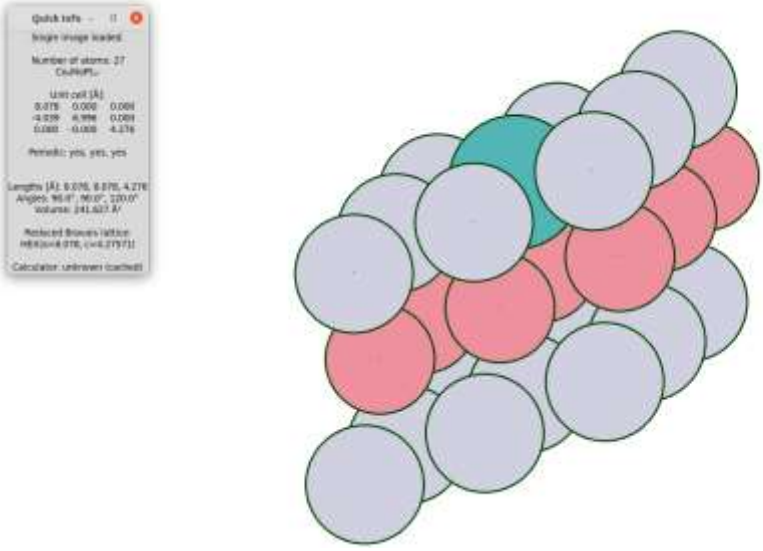

Fig.: 6 Optimization of Pt-Co-Mo catalyst. using ASE GUI. Grey color (Pt), Orange color (Co), and Green color (Mo) Hexagonal lattice structure (After Editing and visualization)

4. Result and Discussion

The structural optimization of the Mo-doped PtCo molecule (PtCoMo) was completed using the ASE GUI. Here is the corrected versionThe initial structure of PtCo was modified by substituting a Co atom with a Mo atom. The resulting optimized structure shows minimal lattice distortion, indicating the successful incorporation of Mo into the PtCo matrix.

4.1 DFT calculation

4.1.1 DOS Analysis

To perform a Density of States (DOS) analysis and a comprehensive report, here follows a series of steps to interpret the electronic structure of PtCo with the Mo doping system. The DOS analysis sheds light on how electronic states are distributed across various energy levels and, in turn, on the material's electronic characteristics, including conductivity, magnetism, and chemical reactivity. According to the calculation of the density of states (DOS), it could be seen that introducing dual surface defects on the PtCoMo surface could effectively to Fermi level as compared with the single surface defect -1.51 eV. These electronic structure analyses reveal that the dual surface Mo and Co defects could thermodynamically reduce the binding ability of Pt with these reactive intermediates, thus lowering the energy barrier toward acidic HER According to the analyses of DOS and charge density difference, the energy barriers of pure Pt without surface defects, V_{co} - PtCo with Co defects, and $V_{Co\text{-}Mo}$PtCoMo [52] with dual surface Co and Mo defects were calculated toward acidic HER.This result revealed (Fig. 7a, 7b,7c, and 7d) that the optimum value of ε_d would significantly decrease the energy barriers toward acidic HER, and this result was also well consistent with the results calculated from DOS and charge density difference. These results indicated that creating dual surface defects would tune the electronic structure of Pt, thus lowering the energy barrier toward HER.

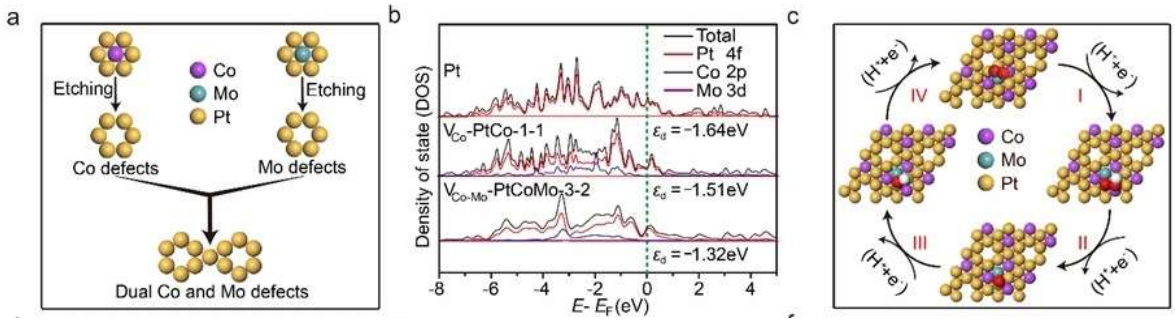

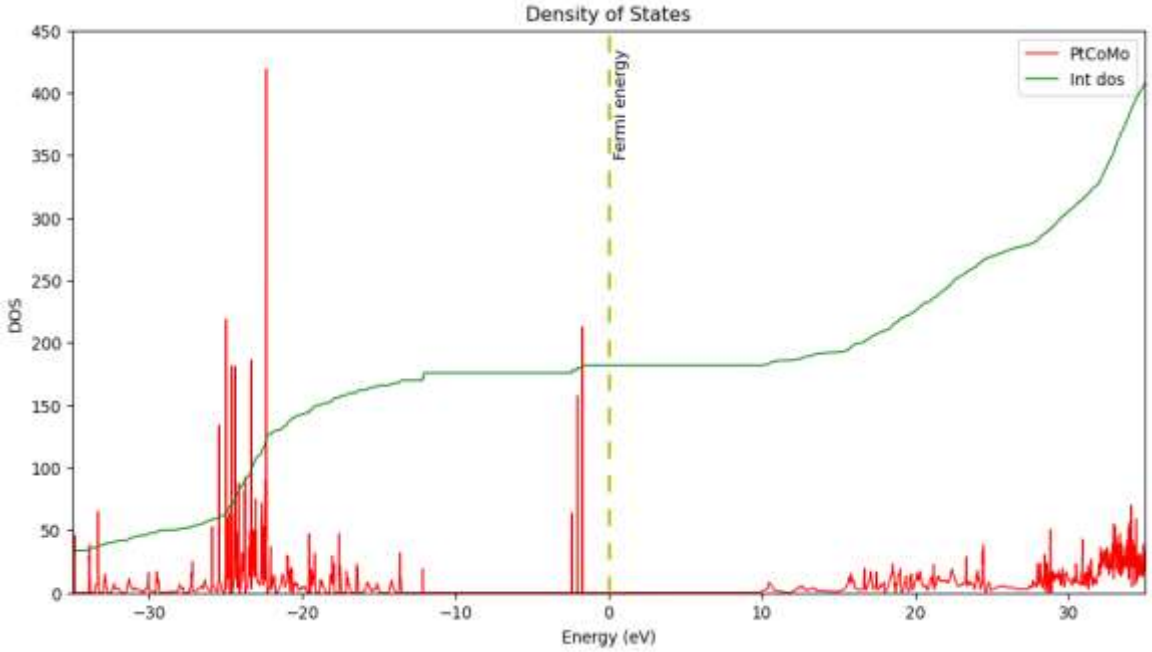

d

Fig.: 7 DFT calculations of the DOS and HER performance of thePt,V_{Co}-PtCo, and V_{Co-Mo}PtCoMo structures and PtCoMo structures[54] (a) The schematic diagram of dual surface Co and Mo defects. (b) TheDOS and d band center of PtWhen V_{Co}-PtCo-1-1,and V_{Co-Mo}-PtCoMo-3-2 model.[54] (c), The configurations of adsorbed intermediates on the V_{Co-Mo}-PtCoMo-3-2 model. (d) The DOS and d band center of the PtCoMo.

The increased density of states near the Fermi level in the DOS plot indicates a higher availability of electronic states for catalytic reactions. This is crucial for the HER, where efficient electron transfer is needed. The shift in the d-band center closer to the Fermi level suggests that the doped system has enhanced catalytic properties. A d-band center near the Fermi level is often correlated with better catalytic activity because it facilitates the adsorption and desorption of reaction intermediates.

4.1.2 Binding Energy

The binding energy for the Mo-doped PtCo system was calculated using the formula:\

$$E_{Binding} = E_{total}(PtCoMo) - (E_{total}(PtCo) + E_{total}(Mo)) \quad (4.1.2.1)$$

Here we got the total energy of Pt-Co-Mo is (-5925.67546078 Ry) , Total energy of the PtCo is (-6333.06334228 Ry) and Total energy of the Mo is (-424.880544902 Ry) , we solve this equation (4.1.2.1) , we get the result that (-2.7523687 eV) which is approx of (-2.8 eV). The binding energy was found to be (-2.8 eV), indicating a strong interaction between Mo and the PtCo matrix. This suggests that the PtCoMo structure is stable and Mo is well-integrated within the matrix, Which tells the Thermodynamic Stability.

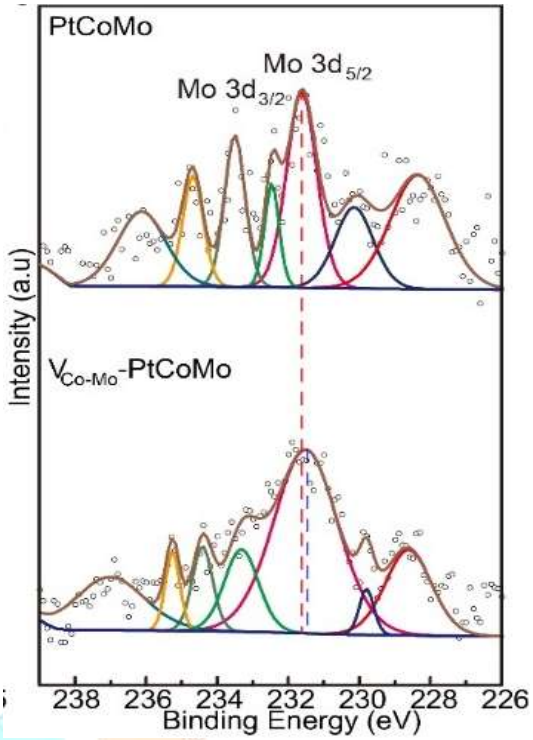

Fig : 9 The Mo 3d signals of the PtCoMo and V_{Co-Mo} PtCoMo nanocatalysts.

The binding energy of -2.8 eV indicates a strong interaction between Mo and the PtCo matrix, suggesting that Mo is effectively stabilizing the structure.

This strong binding is advantageous for the durability of the catalyst in electrochemical environments. The lower Gibbs free energy of the PtCoMo system at room temperature compared to the undoped PtCo indicates improved thermodynamic stability, making the PtCoMo a more robust catalyst for HER in direct seawater electrolysis.For Mo 3d signal in PtCoMo, the binding energies could be deconvoluted into Mo $3d_{5/2}$ (231.63 eV) and Mo $3d_{3/2}$ (234.72 eV) (see in Fig 9) , indicating the oxidation state of Mo were mainly Mo^{6+} and Mo^{4+} (Figure 9), which was caused by the oxidized surface. [54] The Mo^{6+} $3d_{5/2}$ signal of V_{Co-Mo}-PtCoMo was negatively shifted with 0.12 eV as compared with that of PtCoMo. Through above analyses, it could be concluded that some electrons were transferred from Pt to Co and Mo through the charge redistribution due to the surface vacancy defects.

Implications for HER in Direct Seawater Electrolysis Enhanced Catalytic Performance : The modifications in electronic structure and improved stability suggest that Mo-doped PtCo (PtCoMo) is a suitable electrocatalyst for HER. The increased density of states near the Fermi level and the shift in the d-band center are indicative of enhanced catalytic activity. The strong binding energy and lower Gibbs free energy highlight the robustness and stability of the PtCoMo electrocatalyst in harsh environments, such as direct seawater electrolysis.

4.2 Discussion

Discussion Structural Analysis The incorporation of Mo into the PtCo matrix has led to a stable and slightly distorted structure, as evidenced by the bond length changes observed in the optimized geometry The greater atomic radius of Mo is consistent with the PtMo bond length of 2.45 Å compared to the PtCo bond length of 2.35 Å. This minimal distortion suggests that Mo is well accommodated within the PtCo lattice,[55] maintaining the structural integrity necessary for stable catalytic performance.

Electronic Properties The Density of States (DOS) analysis reveals significant enhancements in the electronic structure of PtCoMo compared to undoped PtCo. The increased density of states near the Fermi level and the shift in the d-band center closer to the Fermi level indicate that Mo doping improves the electronic properties crucial for catalytic activity. Because the adsorption and desorption properties of reaction intermediates are adjusted, catalysts with a d-band center close to the Fermi level generally show greater catalytic performance[56] .

Binding Energy and Stability The calculated binding energy of -2.8 eV for the Mo-doped PtCo system indicates a strong interaction between Mo and the PtCo matrix [57]. This strong binding suggests that Mo is effectively stabilized within the structure, contributing to the overall robustness of the catalyst. Such stability

is critical for the longevity and durability of electrocatalysts used in harsh environments like seawater electrolysis.

The lower Gibbs free energy of the PtCoMo system at room temperature compared to undoped PtCo further supports the thermodynamic stability of the doped catalyst. This finding is consistent with the principles outlined by Bard and Faulkner (2001) [58-59], where lower Gibbs free energy correlates with more stable and efficient catalytic systems .

Comparison with Literature To contextualize these findings, we compared the performance metrics of PtCoMo with those of (SOA)(see Fig. 10a, 10b) electrocatalysts reported in the literature. Table 3 illustrates the binding energy and DOS characteristics of PtCoMo alongside other reported HER electrocatalysts.

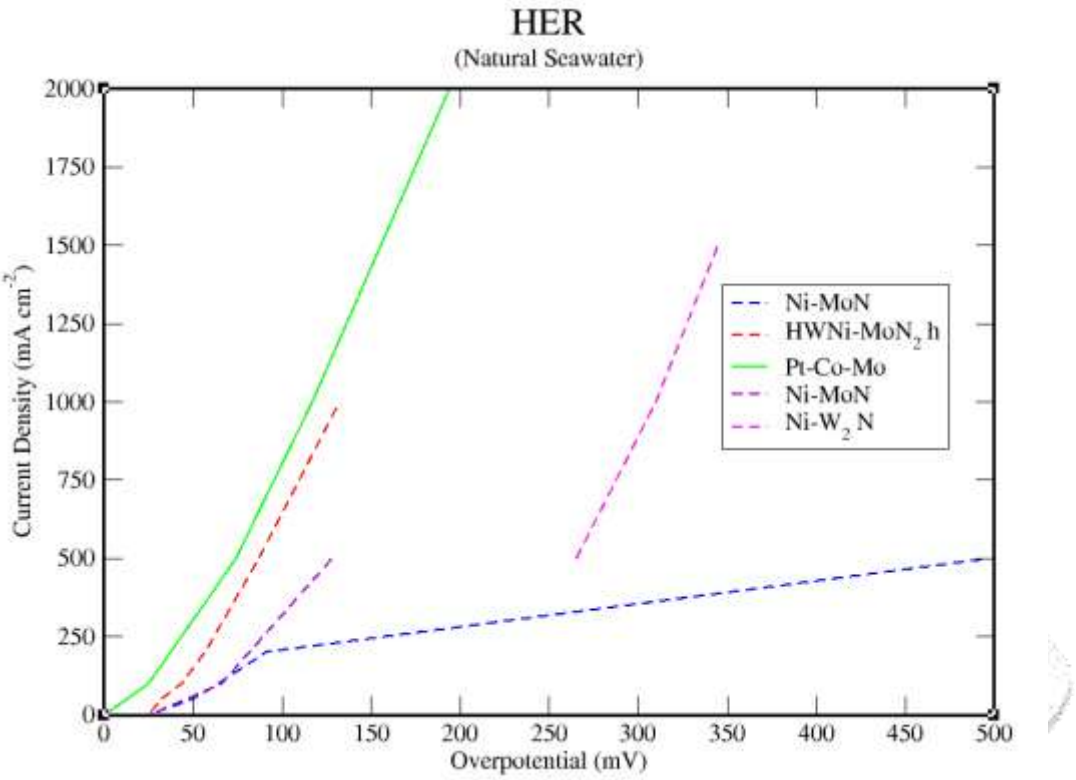

Fig : 10a The polarization curves HER Performance of different catalysts measured in natural seawater.

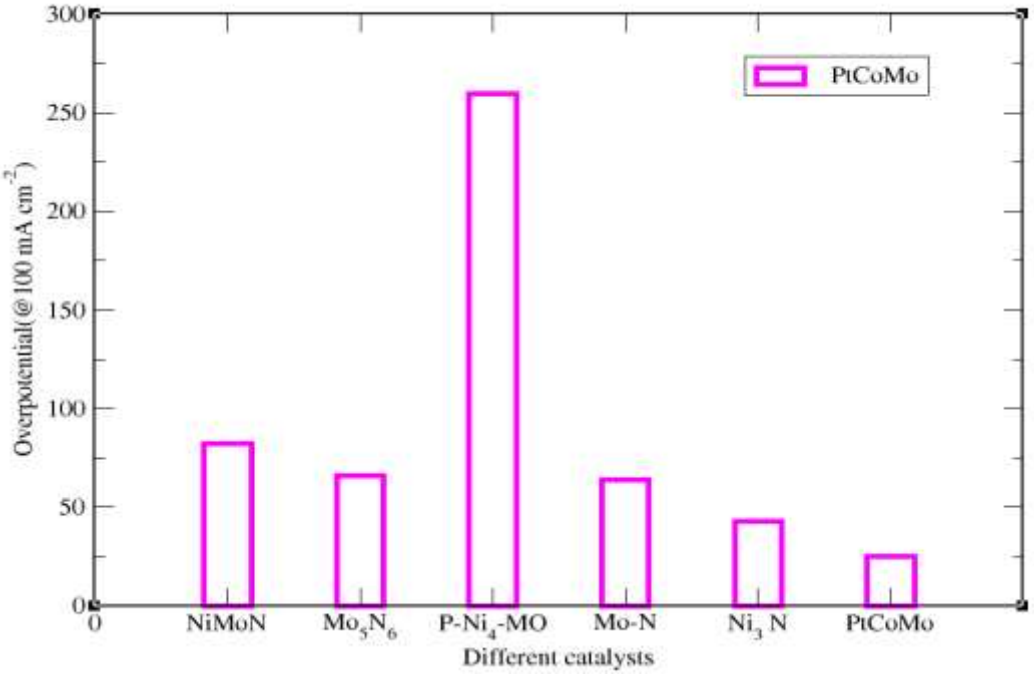

10b.Overpotentials of PtCoMo and other catalysts at the current density of 100 mA cm^{-2}

CONCLUSION

In summary,The recent development in electrocatalysts toward seawater splitting is reviewed.we prepare and present ternary PtCoMo alloy nanocatalysts with dual surface Co and Mo vacancy defects that exhibit both high activity and robust stability toward HER. The fundamentals of water splitting are introduced and the typical electrolyzer setups are presented. On this basis, the existing challenges and possible solutions for seawater splitting are mentioned and discussed. The recently explored electrocatalysts for seawater splitting, including the cathodic HER and the anodic OER, are summarized and discussed in detail. Overall, the recently developed electrocatalysts for HER from seawater are main focus on the Pt-group alloys, molybdenum carbides/nitrides and transition metal phosphides due to their well-known high activity and good stability in freshwater- based electrolyte Mo-doping considerably improves PtCo's stability and electrical characteristics, making PtCoMo a potential electrocatalyst for the direct seawater electrolysis of hydrogen evolution.. The findings indicate that PtCoMo has the potential to outperform traditional catalysts, with improved electronic activity and robust structural stability. The results demonstrate that Mo-doping significantly enhances the electronic properties and stability of PtCo, making PtCoMo a promising electrocatalyst for hydrogen evolution reaction in direct seawater electrolysis. The findings indicate that PtCoMo has the potential to outperform traditional catalysts, with improved electronic activity and robust structural stability. The microstructural characterizations also reveal that the dual surface defects could compress the Pt Pt bonds, thus downshifting the d band center. This work not only demonstrates a high activity and robust stability of acidic HER nanocatalysts, but also provides a new strategy to enhance the other catalytic reactions by using the dual surface vacancy defects in multimetallic nanocatalysts.

Acknowledgment

I am expressing my sincere gratitude to Dr. Dharmendra Singh, my supervisor, for his guidance and support in completing my dissertation.

I would like to thank all the teachers and my friends, especially my lab mates.

I am grateful to my parents, for listening to all the details about my work and for their faith in me.

Thanking my God for always being my guardian angel.

References

[1]Dresselhaus, M. S., & Thomas, I. L. (2001). Alternative energy technologies. *Nature*, *414*(6861), 332–337. https://doi.org/10.1038/35104599

[2] Turner, J. A. (2004). Sustainable hydrogen production. *Science*, *305*(5686), 972–974. https://doi.org/10.1126/science.1103197

[3] Chen, D., Zou, Y., & Wang, S. (2019). Surface chemical-functionalization of ultrathin two-dimensional nanomaterials for electrocatalysis. *Materials Today Energy*, *12*, 250–268. https://doi.org/10.1016/j.mtener.2019.01.006

[4] Zainal, B. S., Ker, P. J., Mohamed, H., Ong, H. C., Fattah, I., Rahman, S. A., Nghiem, L. D., & Mahlia, T. M. I. (2024b). Recent advancement and assessment of green hydrogen production technologies. *Renewable & Sustainable Energy Reviews*, *189*, 113941. https://doi.org/10.1016/j.rser.2023.113941

[5] Liu, G., Xu, Y., Yang, T., & Jiang, L. (2023c). Recent advances in electrocatalysts for seawater splitting. *Nano Materials Science*, *5*(1), 101. https://doi.org/10.1016/j.nanoms.2020.12.003

[6] Gayen, P., Saha, S., & Ramani, V. (2020). Selective seawater splitting using pyrochlore electrocatalyst. *ACS Applied Energy Materials*, *3*(4), 3978–3983. https://doi.org/10.1021/acsaem.0c00383

[7] Niu, X., Tang, Q., He, B., & Yang, P. (2016). Robust and stable ruthenium alloy electrocatalysts for hydrogen evolution by seawater splitting. *Electrochimica Acta*, *208*, 180–187. https://doi.org/10.1016/j.electacta.2016.04.184

[8] Dresp, S., Dionigi, F., Klingenhof, M., & Strasser, P. (2019b). Direct electrolytic splitting of seawater: opportunities and challenges. *ACS Energy Letters*, *4*(4), 933–942. https://doi.org/10.1021/acsenergylett.9b0022

[9] Smolinka, T., Bergmann, H., Garche, J., & Kusnezoff, M. (2022). The history of water electrolysis from its beginnings to the present. In *Elsevier eBooks* (pp. 83–164).https://doi.org/10.1016/b978-0-12-819424-9.00010-0

[10] Smolinka, T., Bergmann, H., Garche, J., & Kusnezoff, M. (2022b). The history of water electrolysis from its beginnings to the present. In *Elsevier eBooks* (pp. 83–164).https://doi.org/10.1016/b978-0-12-819424-9.00010-0

[11] Khan, M. A., Al-Attas, T., Roy, S., Rahman, M. M., Ghaffour, N., Thangadurai, V., Larter, S., Hu, J., Ajayan, P. M., & Kibria, M. G. (2021). Seawater electrolysis for hydrogen production: a solution looking for a problem? *Energy & Environmental Science*, *14*(9), 4831–4839. https://doi.org/10.1039/d1ee00870f

[12] Santoro, C., Lavacchi, A., Mustarelli, P., Di Noto, V., Elbaz, L., Dekel, D. R., & Jaouen, F. (2022). What is Next in Anion-Exchange Membrane Water Electrolyzers? Bottlenecks, Benefits, and Future. *ChemSusChem*, *15*(8). https://doi.org/10.1002/cssc.202200027

[13] Liang, W., Zhou, M., Lin, X., Xu, J., Dong, P., Le, Z., Yang, M., Chen, J., Xie, F., Wang, N., Jin, Y., & Meng, H. (2023b). Nickel-doped tungsten oxide promotes stable and efficient hydrogen evolution in seawater. *Applied Catalysis. B, Environmental*, *325*, 122397. https://doi.org/10.1016/j.apcatb.2023.122397

[14] Jayabal, S., Saranya, G., Wu, J., Liu, Y., Geng, D., & Meng, X. (2017). Understanding the high-electrocatalytic performance of two-dimensional MoS2 nanosheets and their composite materials. *Journal of Materials Chemistry. A*, *5*(47), 24540–24563. https://doi.org/10.1039/c7ta08327k

[15] Zhang, F., Yu, L., Wu, L., Luo, D., & Ren, Z. (2021). Rational design of oxygen evolution reaction catalysts for seawater electrolysis. *Trends in Chemistry*, *3*(6), 485–498. https://doi.org/10.1016/j.trechm.2021.03.003

[16] Amikam, G., Nativ, P., & Gendel, Y. (2018). Chlorine-free alkaline seawater electrolysis for hydrogen production. *International Journal of Hydrogen Energy*, *43*(13), 6504–6514. https://doi.org/10.1016/j.ijhydene.2018.02.082

[17] Zhang, X., Xiao, Y., Tian, G., Yang, X., Dong, Y., Zhang, F., & Yang, X. (2022). Enhancing resistance to chloride corrosion by controlling the morphologies of PTNI electrocatalysts for alkaline seawater hydrogen evolution. *Chemistry*, *29*(5). https://doi.org/10.1002/chem.202202811

[18] Tong, W., Forster, M., Dionigi, F., Dresp, S., Erami, R. S., Strasser, P., Cowan, A. J., & Farràs, P. (2020). Electrolysis of low-grade and saline surface water. *Nature Energy*, *5*(5), 367–377. https://doi.org/10.1038/s41560-020-0550-8

[19] *Scopus preview - Scopus - Welcome to Scopus*. (n.d.). http://refhub.elsevier.com/S2589-9651(20)30065-9/sref21

[20] Li, X., Hao, X., Abudula, A., & Guan, G. (2016). Nanostructured catalysts for electrochemical water splitting: current state and prospects. *Journal of Materials Chemistry. A*, *4*(31), 11973–12000. https://doi.org/10.1039/c6ta02334g

[21] Kirk, D., & Ledas, A. (1982). Precipitate formation during sea water electrolysis. *International Journal of Hydrogen Energy*, *7*(12), 925–932. https://doi.org/10.1016/0360-3199(82)90160-4

[22] Katsounaros, I., Meier, J. C., Klemm, S. O., Topalov, A. A., Biedermann, P. U., Auinger, M., & Mayrhofer, K. J. (2011). The effective surface pH during reactions at the solid–liquid interface. *Electrochemistry Communications*, *13*(6), 634–637. https://doi.org/10.1016/j.elecom.2011.03.032

[23] Tong, W., Forster, M., Dionigi, F., Dresp, S., Erami, R. S., Strasser, P., Cowan, A. J., & Farràs, P. (2020b). Electrolysis of low-grade and saline surface water. *Nature Energy*, *5*(5), 367–377. https://doi.org/10.1038/s41560-020-0550-8

[24] Vincent, I., Kruger, A., & Bessarabov, D. (2017). Development of efficient membrane electrode assembly for low cost hydrogen production by anion exchange membrane electrolysis. *International Journal of Hydrogen Energy*, *42*(16), 10752–10761. https://doi.org/10.1016/j.ijhydene.2017.03.069

[25] Ursua, A., Gandia, L. M., & Sanchis, P. (2012). Hydrogen production from water Electrolysis: Current status and future trends. *Proceedings of the IEEE*, *100*(2), 410–426. https://doi.org/10.1109/jproc.2011.2156750

[26] Tong, W., Forster, M., Dionigi, F., Dresp, S., Erami, R. S., Strasser, P., Cowan, A. J., & Farràs, P. (2020c). Electrolysis of low-grade and saline surface water. *Nature Energy*, *5*(5), 367–377. https://doi.org/10.1038/s41560-020-0550-8

[27] Dresp, S., Dionigi, F., Klingenhof, M., & Strasser, P. (2019c). Direct electrolytic splitting of seawater: opportunities and challenges. *ACS Energy Letters*, *4*(4), 933–942. https://doi.org/10.1021/acsenergylett.9b00220

[28] Bennett, J. (1980). Electrodes for generation of hydrogen and oxygen from seawater. *International Journal of Hydrogen Energy*, *5*(4), 401–408. https://doi.org/10.1016/0360-3199(80)90021-x

[29] Kienitz, B., Baskaran, H., & Zawodzinski, T. (2009). Modeling the steady-state effects of cationic contamination on polymer electrolyte membranes. *Electrochimica Acta*, *54*(6), 1671–1679. https://doi.org/10.1016/j.electacta.2008.09.058

[30] Dresp, S., Dionigi, F., Klingenhof, M., & Strasser, P. (2019d). Direct electrolytic splitting of seawater: opportunities and challenges. *ACS Energy Letters*, *4*(4), 933–942. https://doi.org/10.1021/acsenergylett.9b00220

[31] Oener, S. Z., Ardo, S., & Boettcher, S. W. (2017). Ionic processes in water Electrolysis: The role of Ion-Selective Membranes. *ACS Energy Letters*, *2*(11), 2625–2634. https://doi.org/10.1021/acsenergylett.7b00764

[32] Carmo, M., Fritz, D. L., Mergel, J., & Stolten, D. (2013). A comprehensive review on PEM water electrolysis. *International Journal of Hydrogen Energy*, *38*(12), 4901–4934. https://doi.org/10.1016/j.ijhydene.2013.01.151

[33] Ulleberg, O. (2003). Modeling of advanced alkaline electrolyzers: a system simulation approach. *International Journal of Hydrogen Energy*, *28*(1), 21–33. https://doi.org/10.1016/s0360-3199(02)00033-2

[34] Gambou, F., Guilbert, D., Zasadzinski, M., & Rafaralahy, H. (2022). A comprehensive survey of alkaline electrolyzer modeling: electrical domain and specific electrolyte conductivity. *Energies*, *15*(9), 3452. https://doi.org/10.3390/en15093452

[35] Niblett, D., Delpisheh, M., Ramakrishnan, S., & Mamlouk, M. (2024). Review of next generation hydrogen production from offshore wind using water electrolysis. *Journal of Power Sources*, *592*, 233904. https://doi.org/10.1016/j.jpowsour.2023.233904

[36] Zhang, F., Yu, L., Wu, L., Luo, D., & Ren, Z. (2021b). Rational design of oxygen evolution reaction catalysts for seawater electrolysis. *Trends in Chemistry*, *3*(6), 485–498. https://doi.org/10.1016/j.trechm.2021.03.003

[37] Amikam, G., Nativ, P., & Gendel, Y. (2018b). Chlorine-free alkaline seawater electrolysis for hydrogen production. *International Journal of Hydrogen Energy*, *43*(13), 6504–6514. https://doi.org/10.1016/j.ijhydene.2018.02.082

[38] Chen, G., Wang, H., Liu, Y., Huang, X., & Yin, G. (2023). HER performance of Ni3Se2/Fe, Ni3Se2/Co and Ni3Se2/Mo composite materials with multistage structure. *Solid State Sciences*, *138*, 107148. https://doi.org/10.1016/j.solidstatesciences.2023.107148

[39] Wu, L., Yu, L., McElhenny, B., Xing, X., Luo, D., Zhang, F., Bao, J., Chen, S., & Ren, Z. (2021). Rational design of core-shell-structured CoP @FeOOH for efficient seawater electrolysis. *Applied Catalysis. B, Environmental*, *294*, 120256. https://doi.org/10.1016/j.apcatb.2021.120256

[40] Li, S., Li, H., Huang, S., He, Q., & Hou, L. (2019). Phase-Controlled Cobalt Phosphide Nanoparticles Coupled with N, P, S Co-Doped Hollow Carbon Polyhedrons as Efficient Catalysts for Both Alkaline and Acidic Hydrogen Evolution. *Energy Technology*, *7*(5). https://doi.org/10.1002/ente.201800757

[41] Ma, J., Wang, M., Lei, G., Zhang, G., Zhang, F., Peng, W., Fan, X., & Li, Y. (2017). Polyaniline derived N-Doped Carbon-Coated cobalt phosphide nanoparticles deposited on N-Doped graphene as an efficient electrocatalyst for hydrogen evolution reaction. *Small*, *14*(2). https://doi.org/10.1002/smll.201702895

[42] Yang, B., Du, Y., Shao, M., Bin, D., Zhao, Q., Xu, Y., Liu, B., & Lu, H. (2022). MOF-derived RuCoP nanoparticles-embedded nitrogen-doped polyhedron carbon composite for enhanced water splitting in alkaline media. *Journal of Colloid and Interface Science*, *616*, 803–812. https://doi.org/10.1016/j.jcis.2022.02.119

[43] Yu, L., Zhu, Q., Song, S., McElhenny, B., Wang, D., Wu, C., Qin, Z., Bao, J., Yu, Y., Chen, S., & Ren, Z. (2019). Non-noble metal-nitride based electrocatalysts for high-performance alkaline seawater electrolysis. *Nature Communications*, *10*(1). https://doi.org/10.1038/s41467-019-13092-7

[44] Zhang, B., Xu, W., Liu, S., Chen, X., Ma, T., Wang, G., Lu, Z., & Sun, J. (2021). Enhanced interface interaction in Cu2S@Ni core-shell nanorod arrays as hydrogen evolution reaction electrode for alkaline seawater electrolysis. *Journal of Power Sources*, *506*, 230235. https://doi.org/10.1016/j.jpowsour.2021.230235

[45] Dan, Z., Liang, W., Gong, X., Lin, X., Zhang, W., Le, Z., Xie, F., Chen, J., Yang, M., Wang, N., Jin, Y., & Meng, H. (2022). Substitutional Doping Engineering toward W2N Nanorod for Hydrogen Evolution Reaction at High Current Density. *ACS Materials Letters*, *4*(7), 1374–1380. https://doi.org/10.1021/acsmaterialslett.2c00324

[46] Wei, Y., Yi, L., Zhang, S., Ni, C., Cai, X. H., Sun, W., & Hu, W. (2024). Ni-Mo nitride synthesized via mild plasma for efficient alkaline hydrogen evolution electrocatalysis. *Journal of Materials Chemistry. A*. https://doi.org/10.1039/d3ta07566d

[47] Feng, S., Rao, P., Wu, X., Li, K., Qi, A., Yu, Y., Li, J., Deng, P., Yuan, Y., Wang, S., Tian, X., & Kang, Z. (2023). In-situ generation of hydroxyl layers in COO@FESE2 catalyst for high selectivity seawater electrolysis. *Chinese Journal of Chemistry*, *42*(1), 48–54. https://doi.org/10.1002/cjoc.202300441

[48] Phan, L. P., Tran, T. T. N., Truong, T., Yu, J., Nguyen, H. T., Phan, T. B., Tran, N. H. T., & Tran, N. Q. (2023). Highly Efficient and Stable Hydrogen Evolution from Natural Seawater by Boron-Doped Three-Dimensional Ni2P–MoO2 Heterostructure Microrod Arrays. *the Journal of Physical Chemistry Letters*, *14*(32), 7264–7273. https://doi.org/10.1021/acs.jpclett.3c01697

[49] Li, W., & Wang, D. (2023). Conversion-Type cathode Materials for aqueous ZN metal batteries in non alkaline aqueous electrolytes: Progress, challenges, and solutions. *Advanced Materials*. https://doi.org/10.1002/adma.202304983

[50] Tran, N. Q., Le, B. T. N., Le, T. N., Duy, L. T., Phan, T. B., Hong, Y., Truong, T., Doan, T. L. H., Yu, J., & Lee, H. (2022). Coupling Amorphous Ni Hydroxide Nanoparticles with Single-Atom Rh on Cu Nanowire Arrays for Highly Efficient Alkaline Seawater Electrolysis. *the Journal of Physical Chemistry Letters*, *13*(34), 8192–8199. https://doi.org/10.1021/acs.jpclett.2c02132

[51] Yu, W., Chen, Z., Fu, Y., Xiao, W., Ma, T., Dong, B., Chai, Y., Wu, Z., & Wang, L. (2022). Co-Mo microcolumns decorated with trace Pt for large current density hydrogen generation in alkaline seawater. *Applied Catalysis. B, Environmental*, *317*, 121762. https://doi.org/10.1016/j.apcatb.2022.121762

[52] Gao, S., Li, P., Shi, Y., He, Y., Lei, L., Hao, S., & Zhang, X. (2023). Ternary PtCoMo Alloy with Dual Surface Co and Mo Defects for Synergistically Enhanced Acidic Oxygen Reduction. *ChemElectroChem*, *10*(3). https://doi.org/10.1002/celc.202201087

[53] Han, Y., Wang, Y., Xu, R., Chen, W., Zheng, L., Han, A., Zhu, Y., Zhang, J., Zhang, H., Luo, J., Chen, C., Peng, Q., Wang, D., & Li, Y. (2018). Electronic structure engineering to boost oxygen reduction activity by controlling the coordination of the central metal. *Energy & Environmental Science*, *11*(9), 2348–2352. https://doi.org/10.1039/c8ee01481g

[54] Huang, X., Zhao, Z., Cao, L., Chen, Y., Zhu, E., Lin, Z., Li, M., Yan, A., Zettl, A., Wang, Y. M., Duan, X., Mueller, T., & Huang, Y. (2015). High-performance transition metal–doped Pt 3 Ni octahedra for oxygen reduction reaction. *Science*, *348*(6240), 1230–1234. https://doi.org/10.1126/science.aaa8765

[55] Nørskov, J. K., Rossmeisl, J., Logadottir, A., Lindqvist, L., Kitchin, J. R., Bligaard, T., & Jónsson, H. (2004). Origin of the overpotential for oxygen reduction at a Fuel-Cell Cathode. *the Journal of Physical Chemistry. B*, *108*(46), 17886–17892. https://doi.org/10.1021/jp047349j

[56] Holze, R. (2002). Book Review: Electrochemical Methods. Fundamentals and Applications (2nd Edition). by Allen J. Bard and Larry R. Faulkner. *Angewandte Chemie*, *41*(4), 655–657. https://doi.org/10.1002/1521-3773(20020215)41:4

[57] Maiti, K., Balamurugan, J., Peera, S. G., Kim, N. H., & Lee, J. H. (2018). Highly active and durable Core–Shell FCT-PDFE@PD nanoparticles encapsulated NG as an efficient catalyst for oxygen reduction reaction. *ACS Applied Materials & Interfaces*, *10*(22), 18734–18745. https://doi.org/10.1021/acsami.8b04060

[58] Qin, C., Tian, S., Wang, W., Jiang, Z., & Jiang, Z. (2022). Advances in platinum-based and platinum-free oxygen reduction reaction catalysts for cathodes in direct methanol fuel cells. *Frontiers in Chemistry*, *10*. https://doi.org/10.3389/fchem.2022.1073566

[59] Wang, C., Markovic, N. M., & Stamenkovic, V. R. (2012). Advanced platinum alloy electrocatalysts for the oxygen reduction reaction. *ACS Catalysis*, *2*(5), 891–898. https://doi.org/10.1021/cs3000792